

An Estimation of the Effective Number of Electrons Contributing to the Coordinate Measurement with a TPC

Makoto Kobayashi

*High Energy Accelerator Research Organization (KEK),
Tsukuba, 305-0801, Japan*

Abstract

For time projection chambers (TPCs) the accuracy in measurement of track coordinates along the pad row direction deteriorates with the drift distance (z): $\sigma_X^2 \sim D_X^2 \cdot z / N_{\text{eff}}$, where D_X is the diffusion constant and N_{eff} is the effective number of electrons. Experimentally it has been shown that N_{eff} is smaller than the average number of drift electrons per pad row (\bar{N}). We estimated N_{eff} by means of a simple numerical simulation. The simulation shows that N_{eff} can be as small as $\sim 30\%$ of \bar{N} due to the combined effect of statistical fluctuations in the number of drift electrons (N) and in their multiplication in avalanches.

Keywords:

TPC; Effective Number of Electrons; Spatial Resolution; Diffusion; Simulation

1. Introduction

The spatial resolution of TPCs along the pad row direction is expressed as

$$\sigma_X^2 = \sigma_{0X}^2 + D_X^2 \cdot z ,$$

where σ_{0X} is the intrinsic resolution, D_X takes into account the diffusion, and z is the drift distance. On the other hand the width of pad response is given by

$$\sigma_{\text{PR}}^2 = \sigma_{0\text{PR}}^2 + D_{\text{T}}^2 \cdot z ,$$

with D_{T} being the transverse diffusion constant¹. Let us forget about σ_{0X} and $\sigma_{0\text{PR}}$ here and focus on the z -dependent (diffusion) terms although the origins of the intrinsic terms themselves are of great interest.

D_X^2 is expected to be proportional to D_{T}^2 and expressed as

$$D_X^2 = \frac{D_{\text{T}}^2}{N_{\text{eff}}} ,$$

where N_{eff} is the effective number of electrons. One may naively expect N_{eff} to be the average number of drift electrons per pad row (\bar{N}). In reality, however, N_{eff} is significantly smaller than \bar{N} [1–3]:

$$N_{\text{eff}} = \frac{\bar{N}}{R} ,$$

where R is the reduction factor (> 1).

In what follows an attempt is made to estimate N_{eff} (or equivalently, R) for a typical TPC operated in argon-based gases, by means of a numerical simulation.

¹In presence of axial magnetic field (B) the transverse diffusion constant is given by $D_{\text{T}}(B = 0)/\sqrt{1 + \omega^2 \tau^2}$, where $\omega \equiv eB/m$, the electron cyclotron frequency and τ is the mean free time of drift electrons. D_{T} is related to the diffusion coefficient (D) thorough $D_{\text{T}}^2 = 2D/W$, where W is the electron drift velocity.

2. Expectations

Let us assume:

- Readout pads are aligned along the x axis and charged particles traverse the drift volume of the TPC, in parallel with the readout plane ($z = \text{constant}$) and in perpendicular to the pad rows ($x = \text{constant} = x_0$).
- A charged particle leaves N electrons along its path, to be detected by a single pad row. The initial electron clusters are considered as point-like. The x coordinate of each electron then deviates from x_0 during the drift towards a detection gap² because of transverse diffusion. The standard deviation along the pad row direction at the entrance of the detection gap is denoted by $\sigma_x (\equiv D_T \sqrt{z})^3$.
- Each drift electron gets amplified in the detection gap and the charge (q) is collected by (induced on) the pads. The charge multiplication process (avalanche) of each electron develops independently of those initiated by other electrons and the fluctuation of avalanche size for the i -th electron ($1 \leq i \leq N$) is given by the Polya distribution [4]:

$$P(q_i) = \frac{(1 + \theta)^{1+\theta}}{\Gamma(1 + \theta)} \cdot \left(\frac{q_i}{\bar{q}}\right)^\theta \cdot \exp\left(-(1 + \theta)\frac{q_i}{\bar{q}}\right),$$

where \bar{q} is the average charge and θ is a free parameter determining the shape of distribution.

- The width of the pads is small enough so that the center of gravity of charge distribution on the pads caused by the i -th electron be equal to its arrival position x_i at the entrance of the detection gap.
- The “measured” x coordinate of the track (X) is defined as the charge centroid of the pad response, which is the superposition of the contribution from each of the drift electrons.

Under these assumptions and definitions the track coordinate measured with the pad row is given by a weighted mean of x_i :

$$X = \frac{\sum_{i=1}^N q_i \cdot x_i}{\sum_{i=1}^N q_i}.$$

The expected spatial resolution is readily obtained as follows⁴.

$$\begin{aligned} \sigma_X^2 &= \langle (X - x_0)^2 \rangle \\ &= \left\langle \left(\frac{\sum_{i=1}^N q_i \cdot (x_i - x_0)}{\sum_{i=1}^N q_i} \right)^2 \right\rangle \end{aligned}$$

² The detection gap may be equipped with a multi-wire proportional chamber (MWPC) or a micro-pattern gas detector (MPGD), along with readout pads.

³ Let us ignore displacement of the coordinates caused by the $\mathbf{E} \times \mathbf{B}$ effect near the entrance of the detection gap and possible “quantization effects” on the coordinates due to finite granularity of amplifying elements in the case of MPGD readout.

⁴ From now on, both angle brackets and an over-line denote the average of the quantity in-between or beneath.

$$\begin{aligned}
&= \left\langle \frac{1}{(\sum_i q_i)^2} \left(\sum_i q_i^2 \cdot (x_i - x_0)^2 + \sum_{i \neq j} q_i \cdot q_j \cdot (x_i - x_0) \cdot (x_j - x_0) \right) \right\rangle \\
&= \left\langle \frac{1}{(\sum_i q_i)^2} \left(\langle (x - x_0)^2 \rangle_x \cdot \sum_i q_i^2 + \langle x - x_0 \rangle_x^2 \cdot \sum_{i \neq j} q_i \cdot q_j \right) \right\rangle_q \\
&= \left\langle \frac{\sum_i q_i^2}{(\sum_i q_i)^2} \right\rangle \cdot \langle (x - x_0)^2 \rangle \\
&= \left\langle \frac{\sum_i q_i^2}{(\sum_i q_i)^2} \right\rangle \cdot \sigma_x^2,
\end{aligned}$$

where the symbol $\langle \dots \rangle_{x(q)}$ stands for the average taken over a variable (variables) x (q_i). Hereafter we assume $Q \equiv \sum_{i=1}^N q_i = \text{constant} = N \cdot \bar{q}$, expecting $N \gg 1$. Then

$$\sigma_X^2 = \frac{\sigma_x^2}{N} \cdot \frac{\bar{q}^2}{\bar{q}^2} \equiv \frac{\sigma_x^2}{N} \cdot (1 + f),$$

with $f \equiv \sigma_q^2 / \bar{q}^2$, the relative variance of q .

In fact, N is not a constant and fluctuates according to its probability density function $P(N)$. The expected variance in this case is given by

$$\begin{aligned}
\sigma_X^2 &= \sum_{N=1}^{\infty} P(N) \cdot \frac{\sigma_x^2}{N} \cdot (1 + f) \\
&= \sigma_x^2 \cdot (1 + f) \cdot \sum_{N=1}^{\infty} P(N) \cdot \frac{1}{N} \\
&= \sigma_x^2 \cdot (1 + f) \cdot \left(\frac{1}{\bar{N}} \right) \\
&= \frac{\sigma_x^2}{\bar{N}} \cdot (1 + f) \cdot \bar{N} \cdot \left(\frac{1}{\bar{N}} \right) \\
&\equiv \frac{\sigma_x^2}{N_{\text{eff}}} = \frac{D_{\text{T}}^2}{N_{\text{eff}}} \cdot z, \tag{1}
\end{aligned}$$

where $N_{\text{eff}} \equiv \bar{N}/R$, with $R \equiv (1 + f) \cdot \bar{N} \cdot \bar{N}^{-1}$. It is worth noting that one needs to evaluate \bar{N}^{-1} instead of \bar{N} for the estimation of N_{eff} . The reduction factor (R) is a product of statistically independent quantities: $R = R_q \cdot R_N$, where $R_q \equiv 1 + f$ and $R_N \equiv \bar{N} \cdot \bar{N}^{-1}$. The relative variance of Polya distribution is given by $f = 1/(1 + \theta)$. If we assume $\theta = 0.5$, the frequently used value in wire-chamber simulations, $f = 2/3$, yielding ~ 1.67 for R_q ⁵.

It should be noted, however, that $Q \equiv \sum_{i=1}^N q_i$ has been assumed to be constant for a given number N . The validity of this approximation is checked by a numerical simulation (see the next section). As for the estimation of R_N we rely totally on the simulation.

⁵ When $\theta = 0$ the Polya function gives the Furry (exponential) distribution, which is sometimes used to describe avalanche fluctuations. In that case, R_q is expected to be ~ 2 .

3. Numerical simulation

3.1. Assumptions

The simulation was carried out taking into account the following:

1. **Primary ionization statistics** (Poissonian)

The mean number of primary ionization acts per pad row ($\overline{N_P}$) is assumed to be $N_{CL} \times 0.63 \text{ cm} \times 1.2$, where N_{CL} is the average primary ionization density for minimum ionizing particles [cm^{-1}], 0.63 cm is the pad row pitch (\gtrsim pad length) and the factor 1.2 takes account of the relativistic rise for 4 GeV/c pions (see, for example, fig. 8 of Ref. [5])⁶. We use 29.4 cm^{-1} [6] or 24.3 cm^{-1} [7] for the value of N_{CL} in argon.

2. **Cluster size distribution**

We use the probability density listed in table 2 of Ref. [8] for argon (column (b)). This distribution, combined with the primary ionization statistics mentioned above, generates the probability density function $P(N)$ in Eq. (1).

3. **Diffusion:** fluctuation of x_i (Gaussian)

The *standard* normal distribution is chosen arbitrarily just for simplicity. This defines a dimensionless transverse distance scale.

4. **Avalanche fluctuation**

The Polya type with $\theta = 0.5$. \overline{q} is set arbitrarily to 1.

See Figs. 1–3 for the fundamental distributions. It should be noted that the chamber gas is assumed to be pure argon at NTP.

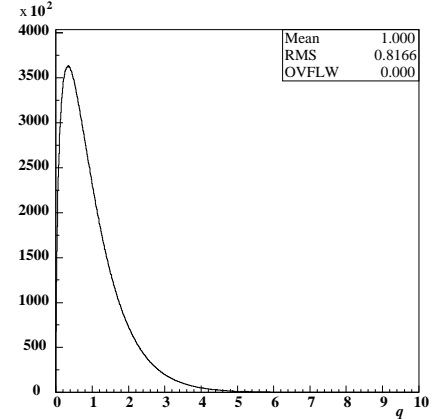
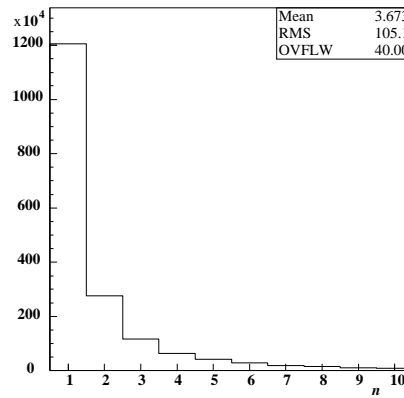
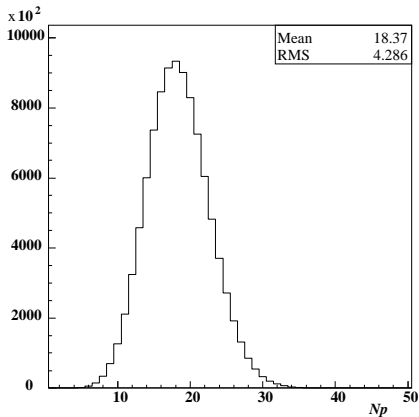


Figure 1: Distribution of the number of primary ionizations (N_P). N_{CL} is assumed to be 24.3 cm^{-1} .

Figure 2: Distribution of the cluster size (n).

Figure 3: Distribution of the avalanche charge (q): the Polya type with $\theta = 0.5$ and $\overline{q} = 1$.

3.2. Results

Table 1 summarizes the results given by the simulation. See also Figs. 4–6 for the relevant distributions. The x coordinate of particle tracks (x_0) is arbitrarily chosen to be 0 in Fig. 4. It should also be recalled that σ_x is set to 1.0 in the simulation.

⁶ The pad row pitch and the incident particles chosen here are typical of those in the experiments of Refs. [2, 3].

Table 1. Summary of the simulation results.

Symbol	Definition	Value	Remarks	Related Figs.
N_{eff}	$\frac{\sigma_x^2}{\sigma_X^2}$	27.7	$N_{\text{CL}} = 29.4 \text{ cm}^{-1}$ $\bar{N} = 71$	—
R	$\bar{N} \cdot \frac{\sigma_X^2}{\sigma_x^2}$	2.57		—
R_N	$\bar{N} \cdot (\frac{1}{N})$	1.59		—
R_q	$\frac{R}{R_N}$	1.62		—
N_{eff}	$\frac{\sigma_x^2}{\sigma_X^2}$	22.2	$N_{\text{CL}} = 24.3 \text{ cm}^{-1}$ $\bar{N} = 71$	Fig. 4
R	$\bar{N} \cdot \frac{\sigma_X^2}{\sigma_x^2}$	3.22		Figs. 4–5
R_N	$\bar{N} \cdot (\frac{1}{N})$	2.00		Figs. 5–6
R_q	$\frac{R}{R_N}$	1.61		—

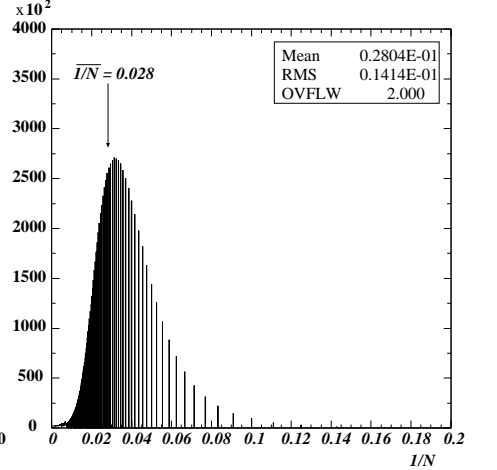
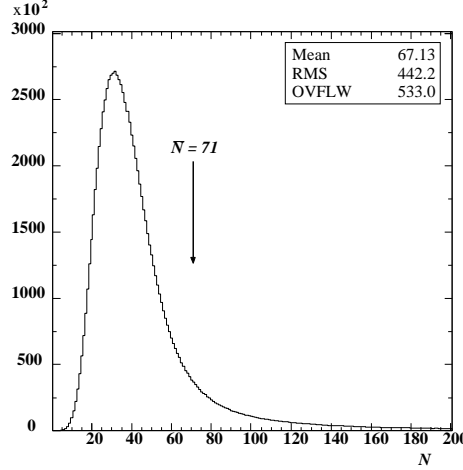
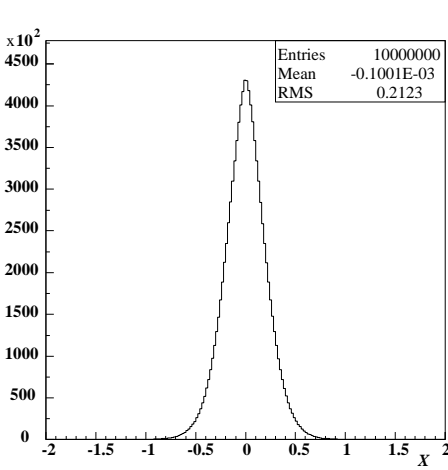


Figure 4: Distribution of the *measured* track coordinates (X).

Figure 5: Distribution of the total number of drift electrons (N).

Figure 6: Distribution of $1/N$.

The simulation results deserve several comments below:

- * We are not sure if the Polya distribution represents the fluctuation in the avalanche size correctly, especially in the case of (cascaded) GEM [9] or MicroMEGAS [10].
- * Granting that the Polya type is an appropriate distribution, the value of parameter θ should depend on gas mixtures and also on the type of detection device: MWPC, GEMs or MicroMEGAS, and its operating high voltages.

- * It may be a bold assumption to suppose no interference between avalanches initiated by different drift electrons when their distances are small.
- * The simulation assumes pure argon as the chamber gas and possible effects of quenchers, such as increase of \overline{N} due to the Penning effect, are not included.
- * The simulation relies on a measurement of cluster size distribution [8], which is a little bit different from the result of a simulation [5].
- * In reality, electron clusters created along a particle path are not point-like and have finite sizes in space (intrinsic track width). However, this hardly affects the z -dependence of spatial resolution (D_X).
- * Drift electrons experience further diffusion in the multiplication region (detection gap). However, this does not contribute to D_X defined in the drift region either.
- * The simulation assumes ideal readout electronics, free from noise, and with a dynamic range wide enough to record tracks containing large cluster(s) and/or large avalanche(s) correctly without saturation of amplifiers or ADC-count overflows.
- * R_q is (approximately) given once the value of θ is fixed. However, $R_N (\equiv \overline{N} \cdot \overline{N^{-1}})$ is sensitive to the cut on the maximum cluster size (n_{\max})⁷ since \overline{N} inevitably depends on n_{\max} while $\overline{N^{-1}}$ is fairly constant over a wide range of assumed n_{\max} ⁸. On the other hand $N_{\text{eff}} \sim 1/\{(1+f) \cdot \overline{N^{-1}}\}$ is rather stable against variation of n_{\max} . It should be noted, however, that N_{eff} as well as R_N depends on $\overline{N_P}$ (N_{CL}) and on the probability densities assigned in the populated region of the cluster size distribution⁹.

4. Summary

We may summarize the results as follows:

- We have carried out a simple numerical simulation of the spatial resolution given by a TPC operated in argon-based gases, taking into account the fluctuations in the total number of drift electrons and in their multiplication in avalanches. The simulation gives 22–28 for the effective number of electrons (N_{eff}) contributing to the coordinate measurement along the pad row, depending on the assumed primary ionization density (N_{CL}). These numbers correspond to 30–40% of the average number of drift electrons per pad row made up of 6-mm-long pads ($\overline{N} \sim 71$).
- Contributions of the two fluctuations, i.e. ionization statistics and avalanche multiplication, to the reduction factor (R) are found to be of comparable size.
- R_q is close to the expected value quoted in section 2 (~ 1.67), justifying, to some extent, the “constant Q ” approximation and the resultant Eq. (1).

⁷ The cluster size distribution has a long tail in proportion to $1/n^2$, with n the cluster size. Therefore a cut has to be applied for large n in order to keep the average total number of electrons (\overline{N}) finite. In the simulation n_{\max} is set somewhat arbitrarily to reproduce \overline{N} consistent with the total ionization density given in Refs. [6, 7] (94 cm^{-1} for minimum ionizing particles).

⁸ This was confirmed by the simulation with several numbers between 10^2 and 10^6 for n_{\max} .

⁹ This was confirmed by intentionally manipulating the cluster size distribution.

- In view of the contribution of diffusion to the spatial resolution it is advantageous to use a gas with a small diffusion constant (D_T), a large electron yield ($\propto \overline{N}$), a high average primary ionization density (N_{CL}) and a small avalanche fluctuation (f)¹⁰, as well as long mean free time (τ) in presence of axial magnetic field. In this respect longer pads are also advantageous in the case of conventional TPCs with discrete pad rows since $\overline{N_P}$ (as well as \overline{N}) is larger, giving a smaller R_N ¹¹, but at the expense of a larger angular pad effect.
- An argument similar to that employed in section 2 is applicable also to the coordinate measurement in the drift direction by substituting Z , z_i and σ_z respectively for X , x_i and σ_x .

The presented method for estimation of the effective number of electrons can be applied for a given gas mixture and for a given amplifying and readout scheme including pad size if the relevant parameters are available.

Acknowledgments

The author would like to thank many colleagues for their continuous encouragement and support. He is especially grateful to Dr. Keisuke Fujii of KEK and Dr. Khalil Boudjemline at Carleton university for fruitful discussions.

References

- [1] R. K. Carnegie, et al., Nucl. Instr. and Meth. A 538 (2005) 372.
- [2] K. Ikematsu, talk presented at the 8th ACFA Workshop on Physics and Detector at the Linear Collider, Daegu, July 2005,
<http://chep.knu.ac.kr/ACFA8/program2.php?sub=Vertex>.
- [3] P. Colas, talk presented at the International Linear Collider Physics and Detector Workshop, Snowmass, August 2005,
<http://alcpg2005.colorado.edu:8080/alcpg2005/program/detector/TRK>.
- [4] G. D. Alkhazov, Nucl. Instr. and Meth. 89 (1970) 155, and references cited therein.
- [5] F. Lapique and F. Piuz, Nucl. Instr. and Meth. 175 (1980) 297.
- [6] F. Sauli, Yellow Report CERN 79-09.
- [7] A. Sharma and F. Sauli, Nucl. Instr. and Meth. A 350 (1994) 470.
- [8] H. Fischle, J. Heintze and B. Schmidt, Nucl. Instr. and Meth. A 301 (1991) 202.
- [9] F. Sauli, Nucl. Instr. and Meth. A 386 (1997) 531.
- [10] Y. Giomataris, et al., Nucl. Instr. and Meth. A 376 (1996) 29.

¹⁰ Notice that $\sigma_X^2 = \sigma_x^2/N_{\text{eff}}$ with $\sigma_x^2 = D_T^2 \cdot z$, and that $N_{\text{eff}} = \overline{N}/(R_q \cdot R_N)$, where $R_q \sim 1 + f$ and R_N is a decreasing function of $\overline{N_P}$ as is expected. We recall that f should depend on the detection device and its operating conditions as well.

¹¹ It should be noted that R_N is greater than unity because of the difference between the mode and the average of N distribution, which is smaller for larger $\overline{N_P}$. See also Table 1 and compare R_N for the different values of N_{CL} .